Taylor & Francis
Taylor & Francis Group

Inhalation Toxicology

International Forum for Respiratory Research

ISSN: 0895-8378 (Print) 1091-7691 (Online) Journal homepage: http://www.tandfonline.com/loi/iiht20

Fiber Deposition in the Tracheobronchial Region: Experimental Measurements

Yue Zhou, Wei-Chung Su & Yung Sung Cheng

To cite this article: Yue Zhou, Wei-Chung Su & Yung Sung Cheng (2007) Fiber Deposition in the Tracheobronchial Region: Experimental Measurements, Inhalation Toxicology, 19:13, 1071-1078, DOI: 10.1080/08958370701626634

To link to this article: https://doi.org/10.1080/08958370701626634

Published online: 06 Oct 2008.

Inhalation Toxicology, 19:1071–1078, 2007

ISSN: 0895-8378 print / 1091-7691 online
DOI: 10.1080/08958370701626634

informa
healthcare

Fiber Deposition in the Tracheobronchial Region: Experimental Measurements

Yue Zhou, Wei-Chung Su, and Yung Sung Cheng
Lovelace Respiratory Research Institute, Albuquerque, New Mexico, USA

Fiber deposition efficiency in the tracheobronchial region was studied by using two human airway replicas. Carbon fibers with a monodisperse diameter of 3.66 μm were delivered into lung casts at the flow rates of 15, 45, and 60 L/min. Deposition efficiencies in each airway bifurcation were obtained individually. Even though the data shows large variability among the bifurcations within the same generation, there is a general trend for the data obtained in these two replicas. Our results show that fiber deposition for carbon fibers increases with the Stokes number, indicating that inertial impaction is the dominant mechanism. Also, fiber deposition in the tracheobronchial region is lower than that of spherical particles at a given Stokes number, and is similar to the deposition found in the nasal and oral airways as reported previously. This finding implies that it is easier for fibers to penetrate the upper respiratory tract and to reach the lower airways as compared to spherical particles. Our measurements are in general agreement with data obtained with asbestos fiber as reported in another study using a hollow airway replica. Our study appears to give a higher deposition efficiency than the results obtained using idealized single symmetrical bifurcation models. This demonstrates, again, the importance of using a realistic airway model, including larynx, to simulate the airway geometry and flow pattern of the human respiratory tract.

Exposures to airborne asbestos and other fiber aerosols increase the incidence of lung cancer, fibrosis, and mesothelioma (Balásházy et al., 2005; Lippman, 1990). Inhalation exposure to asbestos causes (1) asbestosis, a diffuse fibrosis in the alveolar and pleural region of the lung, (2) bronchogenic lung cancer, and (3) mesothelioma in pleura and peritoneum (Bogovski et al., 1973; Selikoff and Lee, 1978). Other mineral fibers such as erionite may have a similar effect on the exposed human population (Baris et al., 1987). Man-made vitreous fibers (MMVFs), including glass fibers, ceramics, and carbides, have replaced asbestos in many applications. Studies conducted in laboratory animals have shown that certain MMVFs may have a biological effect similar to that of asbestos (Kamstrup et al., 2001; Moolgavkar et al., 2001). Although the mechanism of action of these diseases has not yet been clearly elucidated, fiber dimensions and durability play an essential role (Stanton & Wrench, 1972; Timbrell, 1973).

Fiber deposition in human lungs is affected by the interrelationship of four major deposition mechanisms: impaction, interception, sedimentation, and diffusion. Many factors affect the fiber deposition, such as fiber dimensions, lung geometry, and the flow pattern. In most cases, fiber deposition is associated with more than one mechanism. In addition, the orientation of the fibers during flight can also affect the deposition. Theoretical calculation of the fiber deposition in human lungs needs to consider all these factors. Because it is unethical to conduct fiber deposition studies in human volunteers, **a**nimal studies have been used to investigate fiber deposition in lungs. However, there is a large difference in lung geometry between humans and animals, and it is difficult to translate fiber deposition dosimetry obtained in laboratory animals to humans.

Physical models of human airways have been used to study fiber deposition patterns. Simple bifurcation tubes were used to simulate the specific part of the human lung for the lung deposition studies. Myojo alone (1987, 1990) and with his coworker (Myojo & Takaya, 2001) delivered glass fibers, ranging in length from 10 to 100 μm and in diameter from 1.5 to 2.6 μm, into metal bifurcations based on second, third, and fourth generations of Weibel's model A (Weibel, 1963). These studies found that most of the fibers were deposited at the carinal ridge of the bifurcation tubes used, indicating a dominate mechanism of impaction, and that the fibers were oriented parallel to the direction of the flow. However, simple bifurcations are not a good simulation of human tracheobronchial airways because the

Received 9 June 2007; accepted 21 July 2007.
The authors are grateful to W. T. Fan for technical assistance, and V. Fisher for reviewing this article while in manuscript. This project is sponsored by NIOSH grant R01 OH003900.
Address correspondence to Yue Zhou, 2425 Ridgecrest Dr. SE, Albuquerque, NM 87108, USA. E-mail: yzhou@lrri.org

human lung has a complex geometry with an undulating inner surface and asymmetrical bifurcations. Lung casts from human cadavers that replicate the human airway are more realistic models for studying the aerosol deposition in human lungs. Sussman and coworkers (1991a, 1991b) performed a fiber deposition experiment using a human tracheobronchial (TB) replicate hollow cast at high (60 L/min) and low flow rates (15 L/min). They obtained high deposition efficiency with the high flow rate, and found that the deposition was higher in the first few generations than that in the lower generations.

In order to gather more detailed information of fiber deposition in human lungs, a series of experimental studies conducting fiber deposition in human tracheobronchial replicas has been ongoing in our laboratory. Results, including nasal and oral deposition, have been reported (Su & Cheng, 2005, 2006a, 2006b). In this article, we describe local fiber deposition efficiencies in the tracheobronchial region for two realistic human airway replicas as a function of flow rate and fiber dimensions. Carbon fibers of a uniform diameter were used in the study. Using monodisperse-diameter fibers gives one an advantage in investigating the effect of only the fiber's length on deposition. In addition, one of the airway replicas used in this study was also used to study the deposition of spherical particles as previously reported (Cheng et al., 1999; Zhou & Cheng, 2005). The fiber deposition efficiencies of this study can then be compared with those of spherical particle deposition using the same lung replica. We have shown previously that deposition of micrometer-metered-diameter fibers in the human oral and nasal airways is dominated by the impaction mechanism (Su & Cheng, 2005, 2006a, 2006b). We also show that fiber deposition efficiencies in the nasal and oral airways as a function of impaction parameter are lower than those of spherical particles of the same impaction parameter. In this particular study, we wanted to know whether similar results could be observed for deposition in the tracheobronchial airway by comparing our experimental data with the bifurcation study carried out by Myojo and Takaya (2001) and the lung cast study by Sussman et al. (1991a, 1991b).

MATERIAL AND METHODS

Replicas

Two human lung replicas, A and B, including the oral cavity, pharynx, larynx, trachea, and three to four generations of bronchi, were used in the present study as shown in Figure 1. These physical molds of human airways were obtained from dental impressions for the oral cavity and from cadavers for the tracheobronchial region (Cheng et al., 1997, 1999; Smith et al., 2001; Su & Cheng, 2006a, 2006b). There are three major differences between these replicas. The oral cavity of replica A appears to be half open, making a limited air space in the cavity and turning into the oropharynx at a 90° angle. Oral cavity B, however, is fully open, causing a 115° angle in the oropharynx for air to turn. The larynx of replica A has a relatively larger geometry than that of replica B. Moreover, replica B ends with the third generation with only eight terminal tubes, while the replica A has four generations ending with 10 terminals. As

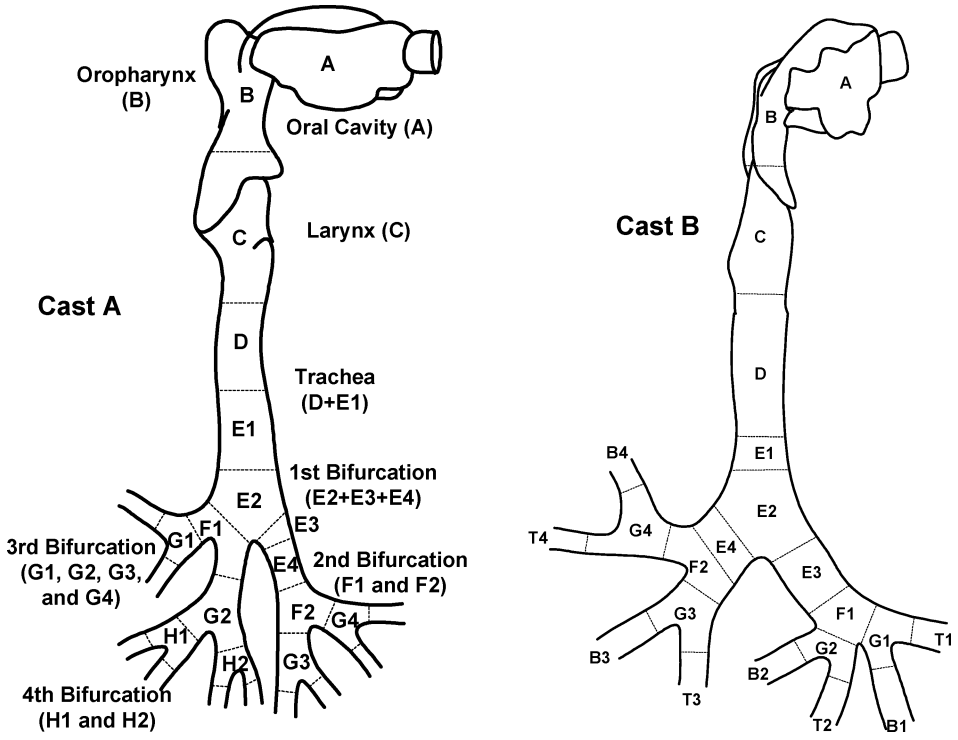

FIG. 1. Schematic of respiratory airway replicas.

TABLE 1
Airway dimensions

	Parent (cm)		Daughter (cm)					
	Length	Diameter	Length	Diameter	Length	Diameter	B angle (°)	P angle (°)
				Cast A				
Trachea, D+E1	7.44	1.58						
1st generation, E2+E3	0.35	1.90	0.32 (to F1)	1.23	1.76 (to F2)	0.71	35	90
2nd generation, F1	0.38	1.23	1.11 (to G1)	0.64	1.24 (to G2)	0.94	84	75
2nd generation, F2	1.26	0.65	0.80 (to G3)	0.30	0.63 (to G4)	0.67	35	75
3rd generation, G1	0.37	0.63	0.50 (to I1)	0.52	0.50 (to I2)	0.54	80	65
3rd generation, G2	0.66	0.90	0.26 (to H1)	0.82	0.26 (to H2)	0.60	35	60
3rd generation, G3	0.24	0.77	0.50 (to I7)	0.60	0.50 (to I8)	0.60	50	70
3rd generation, G4	0.15	0.67	0.50 (to I9)	0.60	0.50 (to I10)	0.55	78	50
4th generation, H1	0.3	0.82	0.50 (to I3)	0.59	0.50 (to I4)	0.64	75	78
4th generation, H2	0.84	0.6	0.50 (to I5)	0.52	0.50 (to I6)	0.49	92	30
				Cast B				
Trachea, D + E1	5.50	1.65						
1st generation, E2 + E3 + E4	1.80	1.52	3.00 (to F1)	1.22	0.55 (to F2)	1.36	57	90
2nd generation, F1	0.60	1.25	0.60 (to G1)	1.15	0.40 (to G2)	0.90	74	81
2nd generation, F2	0.85	1.34	1.50 (to G3)	1.11	0.35 (to G4)	0.90	56	65
3rd generation, G1	0.38	1.15	0.50 (to T1)	0.69	0.50 (to B1)	0.65	73	55
3rd generation, G2	0.25	0.90	0.50 (to T2)	0.68	0.50 (to B2)	0.61	53	14
3rd generation, G3	0.85	1.00	0.50 (to T3)	0.71	0.50 (to B3)	0.64	66	32
3rd generation, G4	0.50	0.90	0.50 (to T4)	0.57	0.50 (to B4)	0.56	90	0

shown in Figure 1, replicas were cut into several segments after the experiment to investigate the local fiber deposition. Detailed dimensions for each part of the tracheobronchial region are listed in Table 1. The measurement of airflow distribution in each terminal tube was described in our previous spherical deposition study (Zhou & Cheng, 2005). Results of deposition studies for spherical particles in cast A were reported (Cheng et al., 1999; Zhou & Cheng, 2005).

Fiber Generation

Conductive carbon fibers (Hercules, Inc., Wilmington, DE) with a monodisperse diameter of 3.66 μm and polydisperse in length (Su & Cheng, 2005) were used in this study. Fibers that met the definition of a fiber, i.e., an elongated particle with an aspect ratio of over 3 with its long axis shorter than 10 μm, were not considered as contributing the deposition results. Fibrous particles generated from a small-scale powder disperser (model 3433; TSI, Inc., St. Paul, MN) were led to an aerosol Kr-85 neutralizer in a chamber where the surface charge of the fiber was neutralized and well mixed with the diluted air. To avoid particle rebounce, with deposited particles resuspended in the airstream again, the inner surface of the replica was coated with silicon oil. Fibers were then passed through the lung replica at 3 inspiratory flow rates of 15, 43.5, and 60 L/min, which cover the breathing rate of a human adult from rest to moderate exercise. Each terminal tube of the replica was connected to a 25-mm mixed cellulose ester membrane filter (GSWP, Milipore Co., Bedford, MA) to collect fibers that passed through the replica. After the aerosol exposure, the replica was cut into segments as shown in Figure 1 and washed with alcohol after each experiment. The alcohol solution was then filtered to obtain the sample slides for fiber counting. Each slide was analyzed with a microscope (200×) for the fiber length distribution and number concentration. More detailed information on experimental setup and the postexperimental procedure is described in Su and Cheng (2006b).

Calculation of Local Fiber Deposition Efficiency

Deposition efficiency of a bifurcation for a certain size fiber can be calculated by the fiber concentration deposited in the bifurcation divided by the concentration before entering the bifurcation. Due to the differences in the lung geometry of replicas A and B, the deposition pattern in the two replicas was different as well (Su & Cheng, 2006a). We used Stokes number in order to compare the deposition efficiency from the same areas of the replicas. The Stokes number is a dimensionless number that include particle size and velocity. High Stokes numbers represent large particles with high travel velocity in a tube, which means the impaction mechanism dominates the particle deposition. For a spherical particle traveling in a tube, the Stokes number is a function of particle diameter, travel velocity, and the diameter of the tube. However, the Stokes number of a fiber is also a function of its orientation in the flow (Cai & Yu,

1988). To simplify the calculation, a fiber equal-volume Stokes number (Stk_v) was used (Zhang et al., 1996):

$$\mathrm{Stk_v} = \frac{\rho_f d_{ev}^2 U}{36\mu R_0} \quad [1]$$

where ρ_f is the density of the fiber; d_{ev} is the diameter of a sphere that has the same volume as the fiber; U is the mean velocity through the parent tube; μ is the air viscosity; and R_0 is the radius of the parent tube. The d_{ev} can be expressed as:

$$d_{ev} = d_f \left(\frac{3}{2}\beta\right)^{1/3} \quad [2]$$

in which d_f is the fiber diameter and β is the fiber aspect ratio.

RESULTS

Deposition in the Tracheal Region

Fiber deposition patterns in the tracheal region strongly depend on the geometry of the oral cavity, oropharynx, and larynx. When airflow passes the oral cavity it turns 90° at the oropharynx to reach the larynx, with its very complex geometry. The flow becomes turbulent when entering the tracheal region, resulting in enhanced deposition in tracheobronchial regions. Figure 2 shows the deposition efficiency of fibers in the trachea as a function of the Stokes number. Because the Stokes number includes the geometry of the cast and the flow rate, the experimental data from different flow rates and casts can be plotted in one figure for comparison. Our results show that fiber deposition data obtained in casts A and B are similar. The deposition efficiency increased as the Stokes number increased, indicating that inertial deposition is the dominant mechanism. Figure 2 also plots the spherical particle deposition in the tracheal region for spherical particles in cast A (Zhou & Cheng, 2005) for a comparison. Fiber deposition efficiency in the trachea is lower than that of spherical particles at a given Stokes number.

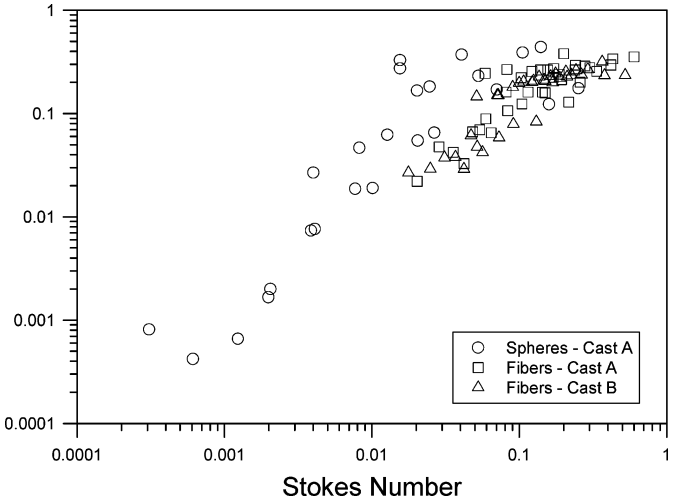

FIG. 2. Comparison of fiber deposition in the trachea for lung casts A and B, and compared with spherical particle deposition in cast A.

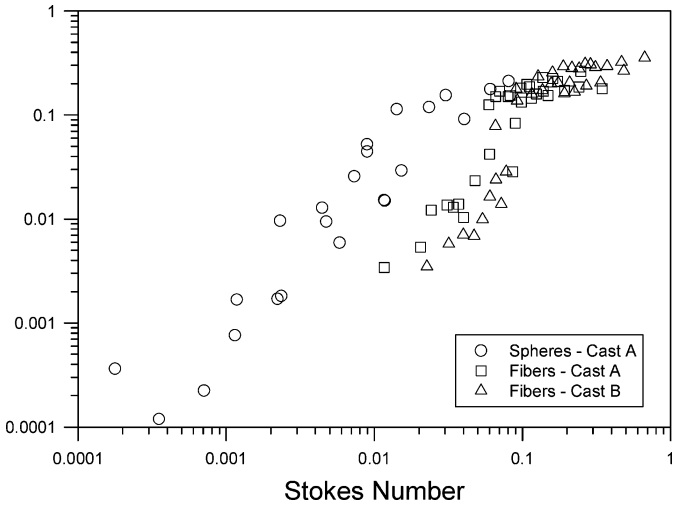

FIG. 3. Fibrous (casts A and B) and spherical (cast A) particle deposition in the first generation.

Deposition in the Upper Bronchial Region

Figure 3 compares fiber deposition efficiency in both casts as well as the deposition of spherical particles in the first generation of the lung casts. In this region, the structures of casts A and B were different. Cast A had an uneven bifurcation with only one daughter tube (Figure 1, E3 and E4). The other daughter tube was too short and was classified as part of the second bifurcation when the deposition was measured. Most fibers were deposited at the bifurcations' carina. Despite the difference in airway structure, the deposition in both casts appears to be quite similar as shown in Figure 3.

The second generations of each cast are of different dimensions and each includes two bifurcations. Figure 4 shows data obtained for both bifurcations of casts A and B, and that for

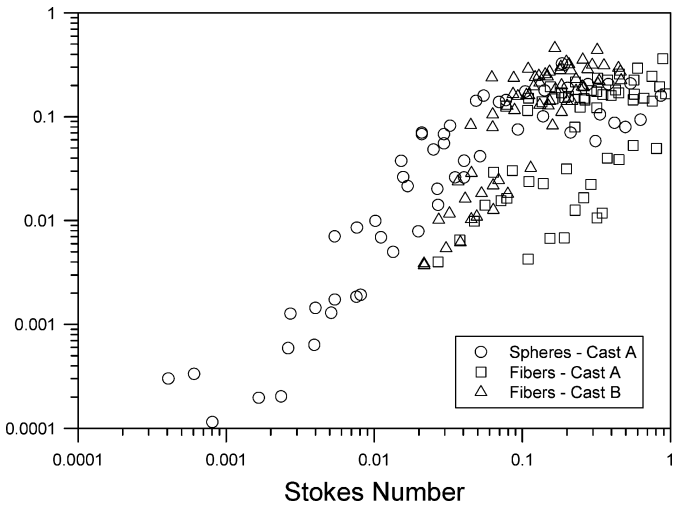

FIG. 4. Fibrous (casts A and B) and spherical (cast A) particle deposition in the second generation.

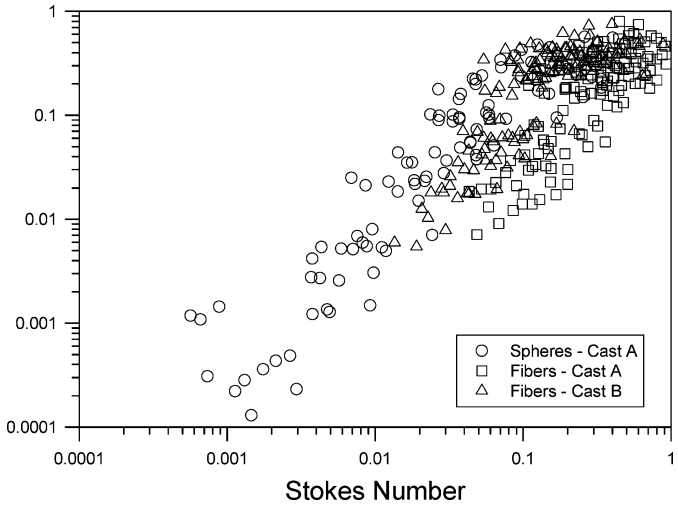

FIG. 5. Fibrous (casts A and B) and spherical (cast A) particle deposition in the third generation.

spherical particles in cast A. Figure 5 shows the fiber deposition efficiency in both casts as well as the deposition of spherical particles for the third generation of cast A. Because there is no fourth generation for cast B and only two bifurcations at the fourth generation for cast A, the comparison for this region was only considered in cast A for fibers and spherical particles as shown in Figure 6.

In general, the deposition was widely scattered in the bronchial airways, even among bifurcations of the same generation. This is similar to spherical deposition data using airway replicas (Cohen et al., 1990; Schlesinger et al., 1982; Zhou & Cheng, 2005). Such deposition could be attributed to the asymmetrical nature of the bronchial airways and the resulting flow pattern. However, the data appear to show a trend of the fiber deposition being higher than that of spherical particles.

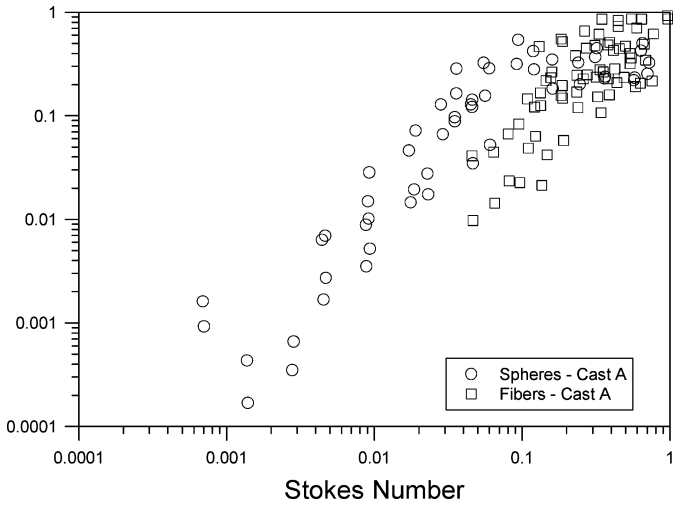

FIG. 6. Fibrous and spherical particle deposition in the fourth generation of cast A.

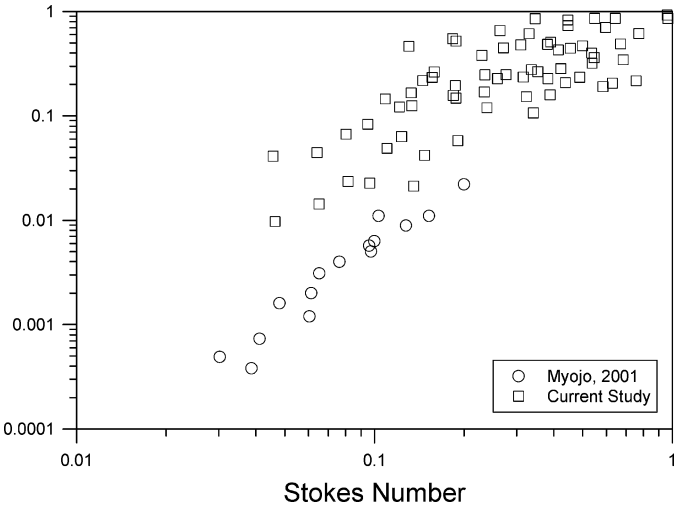

FIG. 7. Fiber deposition efficiency at the fourth generation as a function of the Stokes number compared with the study of Myojo and Takaya (2001).

Comparison to Other Experimental Fiber Deposition Studies

In 1987 and 1990 Myojo, and in 2001 with his coworker, published three papers regarding glass fiber deposition in two bifurcation models (Myojo, 1987, 1990; Myojo & Takaya, 2001). Fibers deposited in these bifurcation models were observed under a scanning electron microscope. The 2001 paper included all results obtained from their studies. Because the dimensions of these two bifurcation models were very close to the bifurcations of the fourth generation of our lung cast A, the results of Myojo and Takaya were only compared with the results of the fourth generation in cast A as shown in Figure 7. The comparison at specific bifurcations is listed in Table 2. Figure 7 shows that deposition obtained from idealized bifurcation models is lower than data obtained using a realistic airway replica.

In 1991, Sussman and his coworkers (1991a, 1991b) published their experimental results for asbestos fiber deposition in a hollow tracheobronchial cast. It is the only fiber deposition study using a human lung cast that we can find in the literature.

TABLE 2
Current study compared with that of Myojo and Takaya (2001) at fourth generation

Parameter	Current study	Myojo and Takaya (2001)
Parent tube (cm)	0.6	0.6 and 0.8
Daughter tube (cm)	0.5	0.4 and 0.6
Fiber type	Carbon	Glass
Fiber diameter (μm)	3.66	1.2
Velocity at parent tube (cm/s)	110	110 and 220

TABLE 3
Current study compared with that of Sussman et al. (1991a)

Parameter	Current study	Sussman et al.
Fiber type	Carbon	Asbestos
Fiber diameter (μm)	3.66	0.3
Flow rate (L/min)	15, 43.5, 60	15, 60

Although the geometry of the lung cast used in their study was different from the one we used, it is also a realistic replica made from human cadaver (Cohen et al., 1990; Schlesinger et al., 1982). In addition, while our replica included the oral airway, larynx, and tracheobronchial airways, their replica included only the tracheobronchial airways with a mechanical larynx. Table 3 lists the experimental conditions for both studies. Because the diameter of asbestos is much smaller than the fiber we used in this study, the comparison was not in the same range of the Stokes number. Figures 8 and 9 show the fiber deposition efficiency as a function of the Stokes number in the trachea and third generation, respectively. Despite the differences in the airway replicas, test material, and experimental conditions, the two sets of data were in general agreement.

Figure 10 summarizes the data for the first through fourth generations of this study and the data of Sussman et al. (1991a, 1991b). The results show, in general, that the deposition of fibers increased with as the Stokes number increased, indicating that inertial impaction is the dominant deposition mechanism. The data in this study seems to be much more scattered than those of Sussman et al. This is due to the method of analysis; Sussman et al. reported the averaged deposition efficiency for each generation, whereas we reported data on each bifurcation.

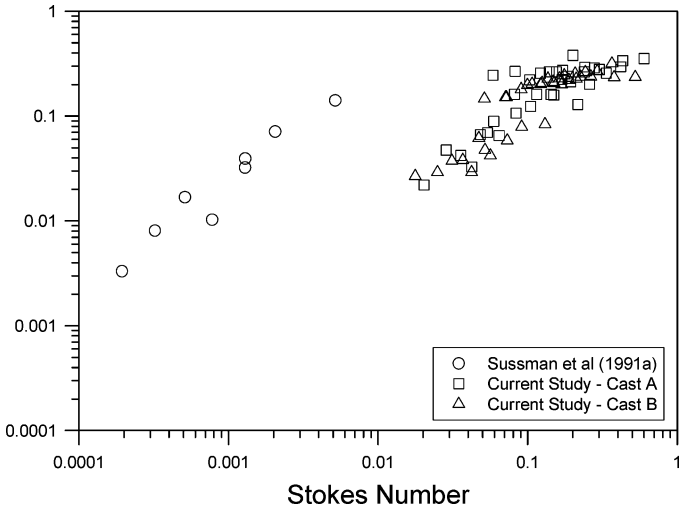

FIG. 8. Fiber deposition efficiency in the trachea as a function of the Stokes number compared with the study of Sussman et al. (1991a).

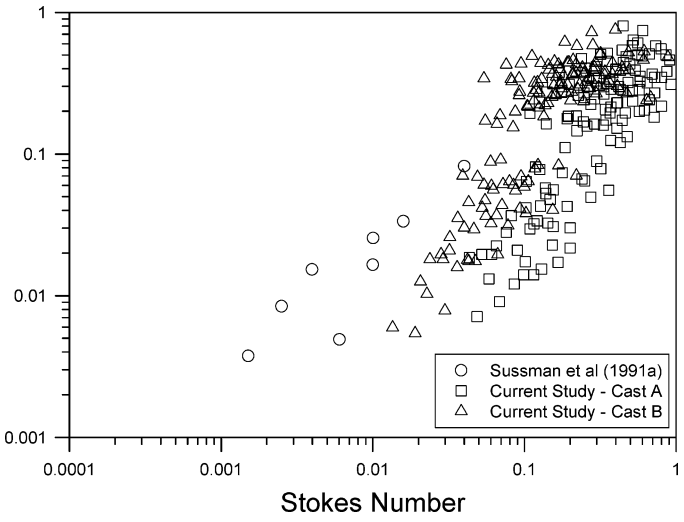

FIG. 9. Fiber deposition efficiency for the third generation as a function of the Stokes number compared with the study of Sussman et al. (1991a).

DISCUSSION

Our results show similar deposition efficiencies between two casts in the tracheal region. Since there is no bifurcation at this region, the flow was relatively simple compared to the lower bifurcated generations. The difference in airway geometry in this region was normalized by the Stokes number. Since the Stokes number is also a function of particle size and flow velocity, it can be used to estimate the effect of the impaction mechanism. Figure 2 shows that fiber deposition efficiency increased with as the Stokes number increased, indicating that impaction is the dominate mechanism for fiber deposition in this region.

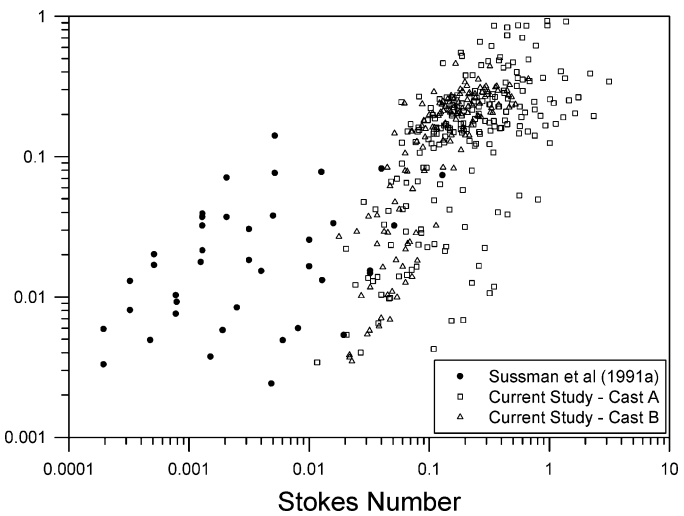

FIG. 10. A summary of deposition data from first to fourth generations of casts A and B as a function of the Stokes number compared with the data of Sussman et al. (1991a).

Fiber deposition efficiencies in the first three generations showed large scatter as a function of the Stokes number. The geometry of each bifurcation can affect fiber deposition. As the Stokes number we used included only the diameter of the parent tube, any other geometry differences, such as the diameter of a daughter tube, the length of the parent and daughter tube, and the angle of the bifurcation, could also affect fiber deposition behavior.

The spherical particle deposition in cast A (Zhou & Cheng, 2005) was also plotted for comparison (Figures 2–6). The fiber deposition efficiency in each generation showed a significant lower value than that for spherical particles. This agrees with the oral and nasal deposition results reported by Su and Cheng (2005, 2006b). This phenomenon indicates that a fiber will pass through the oral/nasal and tracheobronchial regions and reach the lower airway relatively more easily than spherical particles do even if they have the same aerodynamic diameter. In this case, the orientation of the fiber along with the flow might play an important role. Fibers may align themselves to the flow stream when flying in the airways and finally deposit in the alveolar region of the lung (Zhang et al., 1996).

Studies from Myojo (1987, 1990) and with Takaya (Myojo & Takaya, 2001) reported deposition of glass fibers in idealized symmetrical brass bifurcations. The dimensions of their bifurcations are very similar to the fourth generation of our airway replicas. Because the diameter of the fiber we used was larger than theirs, the comparison can only be carried out with the Stokes number ranging from 0.05 to 0.2. The data plotted from our study (Figure 7) shows that the deposition efficiency was higher than that of Myojo's. This may be due to several reasons, including the fact that Myojo's models were symmetrical and had smooth surfaces, which means they were likely to have lower deposition than the realistic airway replicas with rough surfaces. Also the idealized bifurcation models do not include a larynx. Many studies have shown that inclusion of the larynx is important in enhancing deposition in the trachea by simulating the turbulent flow conditions (Martonen et al., 1993; Zhou & Cheng, 2005). It is likely that the turbulence induced by the laryngeal jet could persist in the first few generations of the tracheobronchial airways, resulting in higher deposition efficiency. Despite these differences, Figure 7 shows that the trend of deposition efficiency versus Stokes number for the two sets of data was similar, indicating the same deposition mechanisms.

As previously mentioned, the diameter of asbestos fibers used by Sussman and his coworkers (1991a) was much smaller than what we used. For the tracheal deposition, there was a substantial gap in the Stokes number for the two sets of data, and it is difficult to say whether the data sets are in agreement or not. There is a need for additional deposition data for fiber with a diameter of approximately 1 μm. We are in the process of planning for such studies.

For the deposition in the first to fourth generations of the bronchial airway, there was some overlap of data. In general, deposition efficiencies in these two studies were in agreement. Again, additional data in the range where the Stokes number overlaps would be useful.

CONCLUSIONS

Our results show that fiber deposition for carbon fibers increases as the Stokes number increases, indicating that inertial impaction is the dominant mechanism. Also fiber deposition in the tracheobronchial region is lower than for that of spherical particles at a given Stokes number. These two points are the same as those for deposition in the nasal and oral airways as report previously (Su & Cheng, 2005, 2006a, 2006b), this implies that it is easier for fibers to penetrate the upper respiratory tract and to reach the lower airways. Out measurements are in general agreement with data obtained with asbestos fiber as reported by Sussman et al. (1991). However, additional deposition data for fibers of approximately 1 μm in diameter will be useful in ascertaining the deposition relationship as a function of the Stokes number. Our study appears to give a higher deposition efficiency than the results from Myojo, who used an idealized single, symmetrical bifurcation model. This shows again the importance of using a realistic airway model, including the larynx, to simulate the airway geometry and flow pattern of the human respiratory tract.

REFERENCES

Balásházy, I., Moustafa, M., Hofmann, W., Azoke, R., El-Hussein, A., and Ahmed, A. 2005. Simulation of fiber deposition in bronchial airways. *Inhal. Toxicol.* 17:717–727.

Cai, F. S., and Yu, C. P. 1988. Inertial and interceptional deposition of spherical particles and fibers in a bifurcating airway. *J. Aerosol Sci.* 19:679–688.

Baris, I., Simonato, L., Artvinli, M., Pooley, F., Saracci, R., Skidmore, J., and Wagner, C. 1987. Epidemiological and environmental evidence of the health effects of exposure to erionite fibres: A four-year study in the Cappadocian region of Turkey. *Int. J. Cancer* 39:10–17.

Bogovski, P., Gilson, J. C., Timbrell, V., Wagner, J. C., and Davis, W. 1973. *Biological effects of asbestos*. IARC Scientific Publication No. 8. Lyon, France: IARC.

Cheng, Y. S., Smith, S. M., and Yeh, H. C. 1997. Deposition of ultrafine particles in human tracheobronchial airways. *Ann. Occup. Hyg.* 41(Suppl. 1):714–718.

Cheng, Y. S., Zhou, Y., and Chen, B. T. 1999. Particle deposition in a cast of human oral airways. *Aerosol Sci. Technol.* 31:286–300.

Cohen, B. S., Sussman, R. G., and Lippmann, M. 1990. Ultrafine particle deposition in a human tracheobronchial cast. *Aerosol Sci. Technol.* 12:1082–1091.

Kamstrup, O., Ellehauge, A., Chevalier, J., Davis, J. M. G., McConnell, E. E., and Thevenaz, P. 2001. Chronic inhalation studies of two types of stone wool fibers in rats. *Inhal. Toxicol.* 13:603–621.

Lippman, M. 1990. Effects of fiber characteristics on lung deposition, retention, and disease. *Environ. Health Perspect.* 88:311–317.

Martonen, T. B., Zhang, Z., and Lessmann R. 1993. Fluid dynamics of the human larynx and upper tracheobronchial airways. *Aerosol Sci. Technol.* 19:133–156.

Moolgavkar, S. H., Brown, R. C., and Turim, J. 2001. Biopersistence, fiber length, and cancer risk assessment for inhaled fibers. *Inhal. Toxicol.* 13:755–772.

Myojo, T. 1987. Deposition of fibrous aerosol in model bifurcating tubes. *J. Aerosol Sci.* 18:337–347.

Myojo, T. 1990. The effect of length and diameter on the deposition of fibrous aerosol in a model lung bifurcation. *J. Aerosol Sci.* 21:651–659.

Myojo, T., and Takaya, M. 2001. Estimation of fibrous aerosol deposition in upper bronchi based on experimental data with model bifurcation. *Ind. Health* 39:141–149.

Schlesinger, R. B., Gurman, J. L., and Lippmann, M. 1982. Particle deposition within bronchial airways: Comparisons using constant and cyclic inspiratory flows. *Ann. Occup. Hyg.* 26:47–64.

Selikoff, I. J. and Lee, D. H. 1978. *Asbestos and disease*. New York: Academic Press.

Smith, S., Cheng, Y. S., and Yeh, H. Deposition of ultrafine particles in human tracheobronchial airways of adults and children. *Aerosol Sci. Technol.* 35:697–709.

Stanton, M. F., and Wrench, C. 1972. Mechanisms of mesothelioma induction with asbestos and fibrous glass. *J. Natl. Cancer Inst.* 48:797–821.

Su, W. C., and Cheng, Y. S. 2005. Deposition of fiber in the human nasal airway. *Aerosol Sci. Technol.* 39:888–901.

Su, W. C., and Cheng, Y. S. 2006a. Fiber deposition in two human respiratory tract replicas. *Inhal. Toxicol.* 18:749–760.

Su, W. C., and Cheng, Y. S. 2006b. Deposition of fiber in a human airway replica. *J. Aerosol Sci.* 37:1429–1441.

Sussman, R. G., Cohen, B. S., and Lippmann, M. 1991a. Asbestos fiber deposition in human tracheobronchial cast. I. Experimental. *Inhal. Toxicol.* 3:145–160.

Sussman, R. G., Cohen, B. S., and Lippmann, M. 1991b. Asbestos fiber deposition in human tracheobronchial cast. II. Empirical model. *Inhal. Toxicol.* 3:161–178.

Timbrell, V. 1973. Physical factors as etiological mechanisms. In *Biological effects of asbestos*, IARC Scientific Publication 8. Lyon, France: IARC.

Weibel, E. R. 1963. *Morphometry of the human lung*. New York: Academic Press.

Zhang, L., Asgharian, B., and Anjilvel, S.1996. Inertial and interceptional deposition of fibers in a bifurcation airway. *J. Aerosol Med.* 9:419–430.

Zhou, Y., and Cheng, Y. C. 2005. Particle deposition in a cast of human tracheobronchial airways. *Aerosol Sci. Technol.* 39:492–500.